ENHANCING ACCURACY AND DEPTH-OF-COVERAGE OF ISOTOPICALLY LABELED SAMPLES USING PRECURSOR AND PRODUCT ION RESPONSES FROM DATA INDEPENDENT ANALYZES (DIA)

Waters
THE SCIENCE OF WHAT'S POSSIBLE.™

[1]Roy Martin, [1]Michael Nold, [2]Xin Huang, [2]Shi-Jian Ding, [1]Scott Geromanos
[1]Waters Corporation, Beverly MA, [2]Univ. of Nebraska Medical Center, Omaha NE

INTRODUCTION

Stable isotopically labeled standards have been used effectively in quantitative MS experiments for many years. In the late 90's both Mann[1] & Gygi[2] extended the method to include the analysis of complex protein digests. Though generally accepted the methods' depth of coverage and accuracy of quantitative changes can be compromised by the inherent decrease in dynamic range and increased chimericy afforded by the method itself. The degree to which the data is compromised is proportional to the complexity of the initial sample, its dynamic range as well as the number of different conditions being compared. Following is an explanation illustrating how by increasing the selectivity and specificity of the analytical workflow through in-line serial orthogonal separations, higher mass resolving power and data-independent acquisitions we can achieve greater depth-of-coverage and lower quantitative variation. Additionally since precursor ions' are not selected but aligned with their product ions by retention and drift times each elevated-energy spectrum contains product ions from all peptide variants enabling them to be used in both determining and validating the quantitative change between peptide variants.

METHODS

LC/MS System: 2D nanoACQUITY UPLC® SYNAPT™ G2 HDMS™

Sample Preparation and Loading: SILAC labeling : Human breast cancer cell line MDA-MB-231 was cultured in DMEM-based medium with 10% dialyzed fetal bovine serum. "Heavy" labeling, L-[13C6,15N4]-arginine and L-[13C6,15N2]-lysine, "Light" condition, L-[12C6,14N4]-arginine and L-[12C6,14N2]-lysine. Three proteome mixtures were generated from the heavy (H) and light (L) lysates, total protein weight ratios H/L = 1:1, 1:5, and 1:10. samples were reduced, alkylated and digested in-solution overnight with trypsin .

MS^E Data processing : All datasets were processed and searched with ProteinLynx Global Server (PLGS 2.5).

Peptide and Protein Quantification : Quantitative changes and measurement variations were calculated utilizing the outputted PLGS 2.5 ion lists processed in the UniQuant[3] quantitation software suite.

Workflow

Ion Detection Apex3D.csv	All ions passing the detection criteria are annotated with their retention & drift times, m/z, area, intensity, mass resolution and chromatographic & drift peak width
De-Isotoping Petide3D.csv	Isotope and charge groups are created using isotopic modeling based on each ions' mass resolution, Δ m/z, 1, & Δ drift
Precursor & Product Ion Alignment	Product ions whose apex retention and drift times are within 1/10th the time associated to a precursor ions chromatographic and drift peak widths are aligned to that precursor
Create AMRT	Each ion used to create an AMRT is assigned the same spectrum ID number
Database Search	5 ppm precursors 10 ppm products
Validate IDs	IA physiochemical properties
Add Delta Mass of labeled companion	Calculated the theoretical MH$^+$ of each validated peptides' isotopically labeled labeled companion
Calculate *m/z* for labeled ions	Using the identified peptides' isotope and charge groups as a template calculate the theoretical m/z of each ions labeled companion annotating each with the same apex retention and drift time as the validated peptide
Lookup labeled ions in Apex3D.csv & Peptide3D.csv	Query the calculated *m/z* and retention & drift times (match criteria +/- 5ppm, 0.1 min (t$_r$) and 1 drift bin
Perform peptide and protein quantification and associated statistics	After normalization calculate the quantitative change for all matched ions including all isotopes from all charge groups for both the matched precursor and product ions.

Figure 1

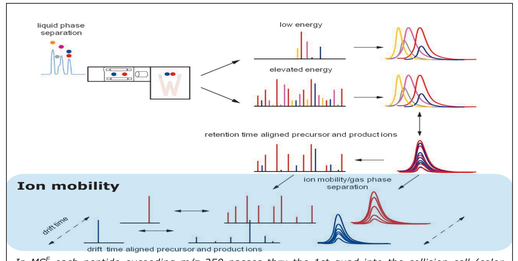

Figure 2

In MS^E each peptide exceeding m/z 250 passes thru the 1st quad into the collision cell (color peaks). The collision energy toggles between a low and elevated-energy state fragmenting all the precursor ions (no precursor ion selection) the resulting fragment ions are then aligned to their parent precursor by their apex retention times. Inclusion of the orthogonal ion mobility separation (HDMS^E) increases selectivity and peak capacity thus decreasing composite and chimeric ion detections.

Figure 3

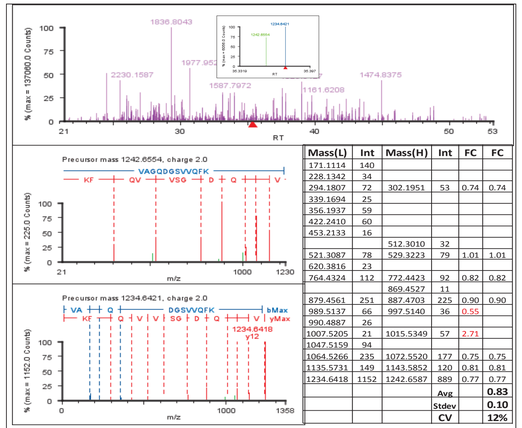

Mass(L)	Int	Mass(H)	Int	FC	FC
171.1114	140				
228.1342	34				
294.1807	72	302.1951	53	0.74	0.74
339.1694	25				
356.1937	59				
422.2410	60				
453.2133	16				
		512.3010	32		
521.3087	78	529.3223	79	1.01	1.01
620.3816	23				
764.4324	112	772.4423	92	0.82	0.82
		869.4527	11		
879.4561	251	887.4703	225	0.90	0.90
989.5137	66	997.5140	36	0.55	
990.4887	26				
1007.5205	21	1015.5349	57	2.71	
1047.5159	94				
1064.5266	235	1072.5520	177	0.75	0.75
1135.5731	149	1143.5852	120	0.81	0.81
1234.6418	1152	1242.6587	889	0.77	0.77
			Avg		0.83
			Stdev		0.10
			CV		12%

Figure 3: *(above): Precursor intensities are recapitulated in the fragment ion intensities. The top panel illustrates the combined monoistopic peptide masses as well as the light/heavy (0.73) ratio for the peptide VAGQDGSVVQFK. The Table on the right illustrates the intensity values and fold changes of paired y" ions of the correct Δ mass. Removing outliers (in red) there are 7 y" ions illustrating a similar fold change to that of their parent precursors (0.83 with a CV of 12%).*

Figure 4: *(right): Fragment ions improve on precursor ratios. The peptide GVQVETISPGDGR from FKB1A_HUMAN demonstrates where UPLC, higher mass resolution, and IMS are not selective enough to accurately assess the quantitative change of the paired precursor between the two conditions. The protein is small (11.8kDa) generating only 6 tryptic peptides (42% obs.). Panel A shows the mobility separated precursors, interferences are marked (*) for the labeled ion at 662.8 m/z (MH^{2+}). Panel B shows the mobility separated fragments, with the series of ions marked. The relative ratios of each paired fragment ion is clear, illustrating a fold change of 0.73 with a CV of ~8%. Ion assignments are shown in Panel C & D.*

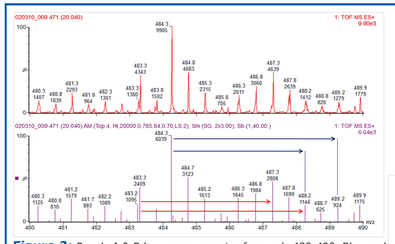

Figure 2: *Panels A & B low-energy spectra from m/z 480-490. Blue and red arrows illustrate how composite signals can be created through the inclusion of isotopically labeled samples. Here the labeled amino acids are (^{13}C ^{15}N K & R). Panel C shows the addition of two labeled peptides, which would have the effect of adding additional peaks to an already populated area of the m/z scale. Panel D is the hypothetical combined spectrum. The red portion of each stick reflects the intensity emanating from the labeled peptide whereby the blue represents that of an unlabeled. Quantitation would be difficult on the combined (chimeric) spectra based on precursor intensity alone. Additional, orthogonal separation would potentially remove these interferences.*

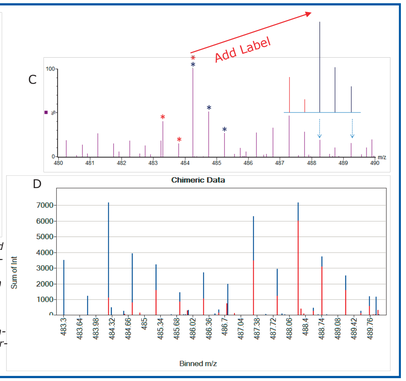

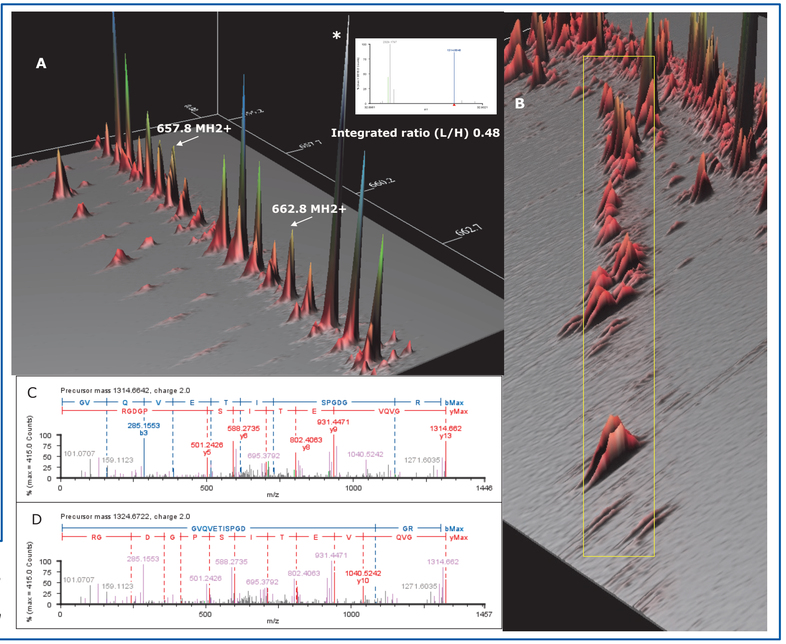

Tables 1 & 2

Precursor Ions

1:5 Mass	1:5 Intensity	1:5 Ratio	1:1 Mass	1:1 Intensity	1:1 Ratio
1688.8236	18944		1688.8308	156956	
1708.8459	27574	0.15	1708.8441	182706	0.88
1584.7531	83272		1584.7504	22056	
1592.7676	9776	0.12	1592.7667	16785	0.75
1968.9132	29143		1968.9132	76639	
1968.9260	33144	0.11	1968.9260	53338	0.70
CV		14%			13%

Product Ions

1:5 Mass	1:5 Intensity	1:5 Ratio	1:1 Mass	1:1 Intensity	1:1 Ratio
1016.4393	5622		1016.4468	3732	
1018.4531	715	0.13	1018.4536	1159	0.68
1109.5073	3650		1109.5085	1871	
1117.5192	579	0.16	1117.5203	736	0.69
1256.5778	4958		1256.5766	1381	
1264.5916	661	0.13	1264.5892	1101	0.85
1384.6373	3630		1384.6357	1495	
			1392.6525	926	0.84
CV		12%			12%

Figure 5

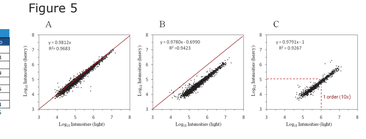

Figure 6

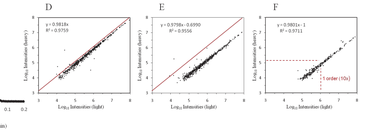

Tables 1 & 2 reflect the calculated MH+ values and intensities of the matched pairs for both the 1:1 and 1:5 sample sets. In addition the ratio of the intensities of the heavy and light pairs as well as their coefficients of variation are also provided. The data presented clearly illustrates that the product ions reflect the same fold change as their parent precursors. Figure 5 Panels A thru C depict log/log plots of the ion intensities of identified and validated product ions whereby Panels D thru F reflect that of their parent precursors. The red line in Panel A depicts an exact match. A simple perusal of the Figure 5 Panels A thru F clearly illustrate how correct and tight the intensity ratios are for the three different datasets. Figure 6 Panels A thru B illustrate respectively, the ppm mass errors for both the precursor and product ions illustrated in Figure 5 Panels A thru F. In addition Panels C & D of Figure 6 represent the differences in retention & drift times of those same paired precursors.

Table 3

	Protein Identification		Protein Quantitation			
			Proteins		Peptides	
	Proteins	Peptides	Number	%[1]	Number	%[2]
H/L = 1:1	808	8119	711	96%	4250	56%
H/L = 1:5	1108	11463	756	75%	3372	31%
H/L = 1:10	1004	10723	537	58%	2541	26%
Overlapped[3] in H/L = 1:1 to 1:5	650	4448	507	84%	2271	55%
Overlapped[3] in H/L = 1:1 to 1:10	629	4249	355	62%	1365	35%
Overlapped[3] in H/L = 1:5 to 1:10	793	5605	407	56%	1784	34%
Overlapped[3] in All three	597	3724	354	64%	1542	46%

[1] Percentage is the number of proteins in SIL-based quantitation divided by the number of identified proteins.
[2] Percentage is the number of peptides in SIL-based quantitation divided by the number of identified peptides.
[3] Overlapped coverage of identified and quantified proteins/peptides is listed accordingly

DISCUSSION

Each of the three peptide mixtures were analyzed by 5 fraction 2D-UPLC-HDMS^E. The resulting data files were processed in PLGS 2.5 utilizing a Tesla 2060 GPU as the microprocessor. The ion detections for each of the 5 fractions were merged into a single ion list for each dilution. The merged datasets were then searched against a forward/reverse concatenated human database with a precursor and product ion mass accuracy of 5 and 10 ppm respectively, for the Pass 1 (only tryptic peptides) increasing to 20 ppm for Pass 2 (VarMods, Missed Cleavages *etc.*). Table 3 reports the number of proteins and peptides identified and quantified as well as the intersection rates for each of the three samples. Figure 6 Panels A-D reflects the mass, retention and drift time differences for all matched pairs. A perusal of the data illustrated in Figure 7 clearly illustrates the validity of the method for quantifying small perturbative differences between cell types including the typical 2—4 fold changes of drug treatments, gene transfections and environmental changes.

With correlations (R^2) between the heavy versus light peptides of 0.9683, 0.9423, and 0.9267 for the H/L = 1:1, 1:5, and 1:10 data, respectively illustrate the precision of the quantitative measurements. The high quality results obtained are a direct response of the methods ability to correctly calculate each ions "true" area through the methods employment of multiple serial orthogonal separation techniques like UPLC, ion mobility, higher mass resolving power, data-independent acquisitions and the unique ability to generate very clean product ion spectra containing all the fragment ions from each of the peptide variants. Inspection of Figure 2 illustrates that when analyzing "systems" samples the presence of an ion occupying any mass sufficient prior to the addition of the isotopically labeled sample(s) is more the rule than the exception. Ignoring this fact will lead to compromise quantitative measurements reflecting high error rates. The ability to increase peak capacity through increased selectivity and specificity will always result in higher quality data.

CONCLUSION

- **Data-Independent Acquisitions can be utilized for quantitative analyzes of SILAC samples**
- **Ion Mobility as a additional orthogonal separation significantly reduces the chimeric nature of "systems" sample**
- **Higher Mass Resolving Powers and UPLC separations further reduce sample complexity**
- **UniQuant is a powerful software tool for elucidating quantitative changes in protein abundance in SILAC labeled samples**

REFERENCES

1. *Ong, S. E., Blagoev, B., Kratchmarova, I., Kristensen, D. B., Steen, H., Pandey, A., and Mann, M. (2002) Stable isotope labeling by amino acids in cell culture, SILAC, as a simple and accurate approach to expression proteomics. Mol. Cell. Proteomics 1, 376– 386*
2. *Everley PA, Krijgsveld J, Zetter BR, Gygi SP. (2004) Quantitative cancer proteomics: stable isotope labeling with amino acids in cell culture (SILAC) as a tool for prostate cancer research, Mol. Cell. Proteomics 3, 729-35*
3. *Huang X, Liu M, Nold M, Geromanos S and Ding S, Quantitative Proteomic Analysis using Stable Isotope Labeling and Data Independent Acquisition, Manuscript in preparation.*

TO DOWNLOAD A COPY OF THIS POSTER, VISIT WWW.WATERS.COM/POSTERS